Published in final edited form as:
Cancer Res. 2015 February 15; 75(4): 742–753. doi:10.1158/0008-5472.CAN-13-3043.

ERK5 is a critical mediator of inflammation-driven cancer

Katherine G. Finegan[*,1], **Diana Perez-Madrigal**[1], **James R. Hitchin**[2], **Clare Davies**[1], **Allan M. Jordan**[2], and **Cathy Tournier**[1,*]

[1]Faculty of Life Sciences, University of Manchester, Manchester, M13 9PT, UK

[2]Drug Discovery Unit Cancer Research UK Manchester Institute, University of Manchester, Manchester, M13 9PT, UK

Abstract

Chronic inflammation is a hallmark of many cancers, yet the pathogenic mechanisms that distinguish cancer-associated inflammation from benign persistent inflammation are still mainly unclear. Here we report that the protein kinase ERK5 controls the expression of a specific subset of inflammatory mediators in the mouse epidermis which triggers the recruitment of inflammatory cells needed to support skin carcinogenesis. Accordingly, inactivation of ERK5 in keratinocytes prevents inflammation-driven tumorigenesis in this model. Additionally, we found that anti-ERK5 therapy cooperates synergistically with existing anti-mitotic regimens, enabling efficacy of sub-therapeutic doses. Collectively, our findings identified ERK5 as a mediator of cancer-associated inflammation in the setting of epidermal carcinogenesis. Considering that ERK5 is expressed in almost all tumor types, our findings suggest that targeting tumor-associated inflammation via anti-ERK5 therapy may have broad implications for the treatment of human tumors.

Keywords

ERK5; tumorigenesis; inflammation; skin

INTRODUCTION

The idea that the immune system influences tumorigenesis was largely overlooked until epidemiological studies identified chronic infection and inflammation as major risk factors for developing various types of cancers (1). Furthermore, in cancers where there is no evidence for an underlying inflammatory reaction prior to tumor formation, malignant cells, unlike their normal counterparts, can attract leukocytes (1). As a result, immune cells create a microenvironment that supports not only the *de novo* development of tumors by promoting the survival and sustained proliferation of cancer cells, but also many aspects of cancer progression, including malignant transformation and angiogenesis (2). Additionally, the resistance of tumor cells to chemotherapeutic agents appears to be enhanced by

[*]**Corresponding author:** Katherine G. Finegan and Cathy Tournier, Faculty of Life Sciences, University of Manchester, Michael Smith Building, Oxford Road, Manchester M13 9PT, UK Tel: +44 161 275 5417; Fax: +44 161 275 5082; k.g.finegan@manchester.ac.uk; cathy.tournier@manchester.ac.uk.

The authors declare no conflict of interest with regard to this publication.

Europe PMC Funders Author Manuscripts

macrophages (3). Consequently, cancer-related inflammation (CRI) is now recognized as one hallmark of cancer (4).

Central to the inflammatory condition associated with tumorigenesis is a complex network of chemokines and cytokines produced by both malignant and myeloid cells in the microenvironment (2). Chemokines and cytokines mediate their effect via the activation of oncogenic transcription factors which have been found constitutively activated in many types of cancers (5). For example, through the activation of nuclear factor κB (NFκB), interleukin (IL) 1α signaling via the IL1 receptor/MyD88 complex establishes a positive feedback loop to reinforce the expression of pro-tumorogenic factors in Ras-expressing keratinocytes (6). Collectively, these observations have advanced our molecular understanding of the pro-tumorigenic function of chemokines and cytokines *in vivo*. In contrast very little is known about the pathogenic signaling mechanisms that initiate the inflammatory reaction.

Mitogen-activated protein kinases (MAPK) are components of core signaling pathways essential for controlling a plethora of cellular processes. In particular, the extracellular-regulated protein kinase 5 (ERK5) is a non-redundant member of this family, which has been implicated in vascular integrity during development and in angiogenesis associated with the formation of tumor xenografts (7). Furthermore, a novel potent and specific ATP-competitive inhibitor of ERK5, XMD8-92, was recently shown to suppress tumor growth through reduced cell proliferation in mice bearing xenografts (8). These findings are highly relevant to human cancer considering that elevated expression of MAPK/ERK kinase 5 (MEK5) and ERK5 in human epithelial tumors correlates with unfavorable prognosis, that includes shorter disease-free intervals, increased risk of metastasis and resistance to chemotherapy (9). However, the interpretation of results obtained from xenograft models can be limited due to immune deficiency of the host. Consequently, a causal relationship between ERK5 and tumorigenesis remained to be rigorously established.

Here, we have developed compound mutant mice with a defect in *erk5* gene expression in epidermal keratinocytes. Using the two-stage chemical carcinogenesis protocol to recapitulate *in situ* the stepwise formation of tumors in the presence of an intact immune system, we have discovered that ERK5 is an essential component of the inflammatory response of the skin associated with tumor formation and maintenance. Accordingly, we demonstrate that anti-ERK5 therapy combined with anti-mitotics more effectively regressed tumors than each treatment alone.

MATERIALS AND METHODS

Genotype determination of mice and tissues

Mice carrying the *erk5*^{fl} allele and the *K14-CreER*^{T2} transgene were identified by PCR on genomic DNA isolated from tail and tissues, as previously described (10, 11). The mouse strains were maintained in a pathogen-free facility at the University of Manchester. All animal procedures were performed under license in accordance with the UK Home Office Animals (Scientific Procedures) Act (1986) and institutional guidelines. In particular, careful clinical examination of the mice was carried out to allow detection of deterioration

of their physical condition associated with the progression of tumors. Animals showing signs of distress were sacrificed before any further deterioration in condition occurred.

Chemical carcinogenesis protocol

Mice were backcrossed into an FVB background. 6 weeks old littermates were subjected to intraperitoneal injection of a non-toxic amount of tamoxifen (200 μg) every day for 5 days. Two weeks later, the shaved backs of the mice received a single application of 7, 12-dimethyl-benzanthracene (DMBA, 25 μg). One week after DMBA, the back skin was treated bi-weekly with 12-O-tetradecanoylphorbol 13-acetate (TPA, 6 μg) for 20 weeks. In Fig. 1E, mice were exposed weekly to a single dose of DMBA (30 μg) for 29 weeks. Tumor burden was recorded (blind counts and photographs) every week for the duration of the experiment. For the tumor regression studies, mice were subjected to the DMBA/TPA protocol for 10 to 16 weeks prior to intraperitoneal injection of tamoxifen (200 μg; every day for 5 days) followed a week later by 3 topical applications of 4-hydroxy-tamoxifen (4-OHT, 100 μg) on alternating days. Alternatively, XMD8-92 (Paterson Institute for Cancer Research, Manchester; 25 μM) was administered topically every other day (3 times, weekly) until the end of the experiments. Age-matched mock treated (acetone) animals were used as controls. Doxorubicin (1.25 mg/kg per mouse) was administered intravenously weekly for 4 consecutive weeks, 1 week after the end of 4-OHT dosing or 1 week after the beginning of XMD8-92 therapy. Bi-weekly TPA treatment was continued for the duration of all regression experiments. When this was combined with XMD8-92, XMD8-92 was applied 30 min prior to TPA. The number of tumors larger than 3 mm in size was recorded (blind counts) every week for the duration of the experiment.

Preparation of epidermises

Skin biopsies were removed and floated dermis-down in 0.25% trypsin-EDTA overnight at 4°C. Epidermises were then separated from the dermis and analyzed as required.

Cell culture

HaCat cells were cultured in DMEM containing 10% FBS, 1% penicillin/streptomycin and 1% glutamine. Where indicated the cells were pre-treated for 30 min with 25 μM XMD8-92 and/or 10 μM caspase 1 inhibitor (Ac-YVAD-CHO; ENZO life sciences).

Immunoblot analysis

Proteins were extracted from cells in RIPA buffer containing inhibitors of proteases and protein phosphatases. Extracts (20 μg) were resolved by SDS-polyacrylamide gel electrophoresis (SDS-PAGE) and electrophoretically transferred to an Immobilon-P membrane (Millipore, Inc.). The membranes were incubated with 3% non-fat dry milk or BSA at 4°C for 60 min and probed overnight with antibodies (1:1000) to ERK5 (Upstate), human IL1β (R and D systems), mouse IL1β (R and D systems) or cleaved caspase 1 (Cell Signaling). Tubulin (Sigma) or actin (Sigma) were used to monitor protein loading. Immunecomplexes were detected by enhanced chemiluminescence with immunoglobulin G coupled to horseradish peroxidase as the secondary antibody (Amersham-Pharmacia).

Protein kinase assay

Endogenous ERK5 was immunoprecipitated from cellular or epidermal extracts in triton lysis buffer (TLB; 20 mM Tris pH 7.4, 137 mM NaCl, 2 mM EDTA, 1% Triton X100, 25 mM β glycerophosphate, 10 % glycerol, 1 mM orthovanadate, 1 mM phenylsulphonyl fluoride, 10 μg/ml leupeptin, 10 μg/ml aprotinin) using an antibody to ERK5 (Upstate). Immunecomplexes were washed twice with TLB and twice with kinase buffer (25 mM HEPES pH 7.4, 25 mM β-glycerophosphate, 25 mM $MgCl_2$, 2 mM DTT, 0.1 mM orthovanadate) prior to being incubated at 30°C for 20 min in kinase buffer containing 50 μM [γ-^{32}P] ATP (10 Ci/mmol) and 1 μg of GST-MEF2C. The reactions were terminated by addition of Laemmli sample buffer. Radioactivity incorporated into the recombinant protein was quantified after SDS-PAGE by PhosphoImager analysis.

ELISA assay

Release of mature IL1β into culture medium was measured using a specific sandwich-type enzyme-linked immunoabsorbent assay (ELISA) (Ready Set Go, Human Interleukin-1 β kit, eBioscience) according to the manufacturer's instructions.

Caspase 1 activity assay

Cellular or epidermal extracts were prepared in caspase buffer (10 mM HEPES pH 7.5, 150 mM NaCl, 2 mM EDTA containing 0.5% NP40). Extracts were incubated with 100 μM YVAD-AMC caspase 1 specific fluorogenic substrate (ENZO lifesciences) for 1 h. Cleavage of the substrate was measured by spectrofluorometer.

Histological and immunohistochemical analyses

Freshly isolated skin biopsies and tumors were fixed in 4% paraformaldehyde, dehydrated and embedded in paraffin. 5 μm thick sections were cut. For histological analysis, sections were stained with haematoxylin and eosin (HE). For immunohistochemistry, sections were deparaffinized, rehydrated, and treated in boiling sodium citrate buffer (10 mM pH 6.0) for 10 min to unmask antigens. Endogenous peroxidase activity was quenched by treating the slides with 0.3% hydrogen peroxide for 10 minutes. Sections were blocked in PBS containing 3-10% goat serum and 0.1% Triton X100 for 1 h at room temperature prior to being incubated overnight at 4°C with primary antibodies (1:100) to ERK5 (Eurogentec), IL1β (R and D systems) or MPO (Thermo-scientific). The following day the slides were rinsed in PBS and incubated at room temperature for 1 h with secondary biotinylated antibodies. The slides were processed using the ABC detection kit (Vector Laboratories). The presence of the antigens were revealed using the Vector® SG (gray) or diaminobenzidine (DAB, brown) peroxidase substrate kit (Vector Laboratories) and counter stained with nuclear red or with haematoxylin (blue). For bromodeoxyuridine (BrdU) staining, the mice were injected with 500 mg/kg BrdU and sacrificed 1 h or 2 h later. Immunohistochemistry was performed using a mouse monoclonal antibody to BrdU (Dako). For mast cell staining, sections were incubated for 5 minutes in toluidine blue stain (0.1% toluidine blue O (Sigma), 1% NaCl, pH 2.5). All slides were viewed using the Axioplan2 microscope.

Quantitative real-time PCR

Total RNA was isolated from cells or epidermises using the Trizol™ reagent and cDNA synthesis carried out, as previously described (12). Quantitative real-time PCRs were performed using the SYBR Green I Core Kit (Eurogentec). Sequences of the forward and reverse primers are indicated in the Supplemental Data available with this article online (Supplementary Table 1). PCR products were detected in the ABI-PRISM 7700 sequence detection systems (Applied Biosystems). Results were analyzed using the $2^{-\Delta\Delta G}$ method. The level of expression of mRNA was normalized to *actin* mRNA.

Statistical analysis

Statistical significance was determined using two-tailed student's t test or ANOVA (one- or two-way) depending on the type of data. $*p < 0.05$ was taken to be statistically significant. ns, indicates no statistical difference. For all mouse tissue experiments, images are representative of cohorts of at least 3 mice.

RESULTS

Inactivation of ERK5 in the skin prevents carcinogen-induced tumorigenesis

Mice lacking *erk5* die before birth (13). To circumvent this early lethality and permit the study of the pathological function of ERK5, we developed a mouse model in which the *erk5* gene was flanked with LoxP sites (referred to as the *flox* (*fl*) allele; 10). Homozygous $erk5^{fl}$ mice expressing Cre fused to a mutated form of the ligand-binding domain of the estrogen receptor ($CreER^{T2}$) under the control of the keratin 14 (K14) promoter (14), were generated. Immunoblot analysis demonstrates that this system allows the specific ablation of ERK5 in the epidermis following injection of the mice with tamoxifen (Fig. 1A and B). Immunostaining of skin sections with an antibody to ERK5 confirmed the absence of ERK5 in the epidermis of $K14\text{-}CreER^{T2};erk5^{fl/fl}$ mice treated with tamoxifen (Fig. 1C). We verified that a control IgG antibody produced no staining under the same experimental conditions (data not shown). The loss of ERK5 in adult mice did not cause any obvious morphological defect, suggesting that ERK5 was not required for skin homeostasis (Fig. 1C). In subsequent experiments, $erk5^{fl/fl}$ and $K14\text{-}CreER^{T2};erk5^{fl/fl}$ animals injected with tamoxifen will be referred to as $erk5^{wt}$ and $erk5^{\Delta epidermis}$ animals, respectively.

To examine the role of ERK5 in tumorigenesis, mice were subjected to the classical two-stage chemical carcinogenesis protocol which gives rise to skin papillomas (15). This simple and highly reproducible system is particularly suited to explore the mechanism of epithelial cancer-associated inflammation because the repeated treatment of the mouse skin with TPA recapitulates a persistent and non-resolving inflammation that promotes the clonal expansion of keratinocytes harboring oncogenic Ha-*ras* mutation (caused by a single, cutaneous application of the genotoxic carcinogen DMBA) (16). Importantly, resolution of inflammation via cessation of TPA treatment causes significant inhibition of tumor growth, as well as frequent spontaneous tumor regression (16). We discovered that tumor burden (number of tumors per mouse) was markedly decreased in the absence of ERK5 (Fig. 1D). In fact, papillomas that developed on the back skin of $erk5^{\Delta epidermis}$ animals were

genotypically wild type. This was predicted since deletion of *floxed* genes following tamoxifen-induced Cre expression does not occur with 100% efficiency.

Additionally, we observed that the malignant conversion of papillomas, which occurred at a frequency ≤ 5-10%, was restricted to $erk5^{wt}$ mice. However, it is possible that malignant tumors in the $erk5^{\Delta epidermis}$ group may have remained undetected, simply because of the low overall total tumor number. Therefore, to assess the role of ERK5 in malignancy, we compared the effect of the repeated treatment of $erk5^{wt}$ and $erk5^{\Delta epidermis}$ animals with DMBA alone (Fig. 1E). This complete carcinogenesis protocol leads directly to the formation of predominantly invasive squamous cell carcinomas (SCC) (17). As with the DMBA/TPA model (Fig. 1D), the absence of ERK5 caused a marked decrease in tumor burden upon exposure to DMBA (Fig. 1E). SCC formation was significantly delayed in *erk5*-deleted skin, with the majority of tumors detected in $erk5^{\Delta epidermis}$ mice significantly smaller than in wild type littermates (Fig. 1E). Together, these results clearly demonstrate that ERK5 is required for the development of malignant skin cancer.

To test whether the resistance of ERK5-deficient mice to tumorigenesis could be attributed to a cell proliferation defect, we performed a short time course analysis of TPA exposure. Epidermal cell proliferation was maximally induced 24 h after a single application of TPA on the dorsal skin of the wild type mice, as demonstrated by a 10-fold increase in the number of BrdU positive cells (Fig. 2A and B). This was significantly impaired in the absence of ERK5 (Fig. 2A and B). However, 6 h after TPA exposure, we did not observe any marked difference in the number of BrdU positive cells between wild type and ERK5-deficient epidermises (Fig. 2B). Instead, by this time, the mutant skin displayed a noticeably lower number of infiltrating cells in the dermis compared to wild type controls (Fig. 2C). This indicated that the proliferative defect displayed by *erk5*-deleted keratinocytes was preceded by a failure of the mutant epidermis to respond to inflammatory stimulation.

Cutaneous inflammation is defective in $erk5^{\Delta epidermis}$ mice

To confirm the requirement of ERK5 in mediating the inflammatory response of the skin to TPA, we examined the effect of epidermal *erk5* gene deletion on neutrophil infiltration into the dermis. Neutrophils rapidly migrate to the skin exposed to TPA and impaired neutrophil recruitment is sufficient to prevent TPA-induced cutaneous inflammation, hyper-proliferation and papilloma formation (18, 19). Accordingly, the number of neutrophils (MPO-positive cells) in skin sections of $erk5^{wt}$ mice increased 10-fold 6 h after TPA treatment and 16-fold after 24 h (Fig. 2D). This effect was significantly reduced in the absence of ERK5, with only a 4- to 5-fold increase in neutrophil number detected in $erk5^{\Delta epidermis}$ animals exposed to TPA for 6 h or 24 h (Fig 2D). A similar defect was observed in skin sections of mice treated with DMBA/TPA for 20 weeks (25-fold increase in neutrophil number in wild type skin, 5- to 6-fold increase in mutant skin).

Two major neutrophil chemoattractants produced by keratinocytes, namely chemokine (C-X-C motif) ligand 1 (CXCL1) and CXCL2, can trigger the recruitment of neutrophils in the mouse skin (20). We confirmed that TPA induced a transient up-regulation of *CXCL1* and *CXCL2* transcripts in the epidermis, with a maximum after 6 h (Fig. 2E). This effect was abolished in the absence of ERK5, consistent with decreased number of neutrophils

trafficking through the dermis of the mutant skin (Fig. 2D and E). Furthermore, *erk5*$^{\Delta epidermis}$ mice were resistant to cutaneous chronic inflammation caused by repeated long term TPA exposure (Fig. 2F). The establishment of chronic inflammation in the wild type skin subjected to the DMBA/TPA protocol for 10 and 20 weeks is demonstrated by the accumulation of resident mast cells in the dermis prior to papilloma formation, and in the tumor stroma (Fig. 2F). Together, our results are consistent with evidence that neutrophil recruitment is a pre-requisite to the establishment of a chronic inflammatory microenvironment and that mice deficient in mast cells are resistant to skin carcinogenesis (21).

To further characterize the requirement of ERK5 in CRI we analyzed the expression pattern of a panel of inflammatory mediators implicated in tumorigenesis. We found that ERK5 was required for TPA-induced *IL1*α and *IL1*β mRNA expression and for the up-regulation of *cyclooxygenase-2* (*COX-2*), a downstream effector of IL1 (22) (Fig. 3A). Prostaglandin E2 (PGE2) is the predominant COX-2 derived product in the skin. It acts by binding to its cognate G-protein coupled receptors, namely EP1-4. Although all EP receptors, except EP3, participate to skin tumor development, genetic analyses have suggested an essential role of EP2 in tumorigenesis (23). Here, we confirmed that TPA increased the expression of *EP1* and *EP2*, but not *EP3*, mRNA in the epidermis (Fig. 3A and Supplementary Fig. S1). Consistent with its very low level of expression in the skin (24), the *EP4* transcript was undetectable (data not shown). More importantly, TPA-induced *EP2* expression was abolished in the absence of ERK5 (Fig. 3A), while no marked difference was detected in the level of *EP1* between wild type and *erk5*-deleted epidermises, under basal or stimulated conditions (Supplementary Fig. S1). Likewise, TPA-mediated increased *TNF*α and *IL6* mRNA expression was independent of ERK5 (Fig 3A), thereby demonstrating the selective requirement of ERK5 signaling in controlling a specific subset of inflammatory mediators.

These results establish ERK5 as a novel regulator of cutaneous inflammation via the up-regulation of neutrophil chemoattractants and of the IL1-COX-2 pathway. CXCL-mediated dermal recruitment of neutrophils and COX-2-generated PGE2 signaling through the EP2 receptor constitute potentially important mechanisms by which ERK5 contributes to skin tumorigenesis.

Regulation of IL1β by ERK5

IL1α and IL1β are synthesized as pro-forms. While IL1α is active as a membrane precursor, caspase-1 mediated cleavage of pro-IL1β is required for IL1β to be active as a secreted form (25). Once cleaved, IL1β is quickly released into the microenvironment (26). We found that the intracellular level of cleaved IL1β was significantly lower in the mutant epidermis compared to wild type samples (Fig. 3B). Consistent with the requirement of ERK5 for mediating the proteolytic cleavage of pro-IL1β, *erk5*-deleted epidermises were resistant to TPA-induced caspase 1 activation (Fig. 3C). Elevated caspase 1 activity in the wild type skin exposed to TPA is indicative of rapid turn-over of the pro-form and subsequently, secretion of the cleaved fragment. This dynamic process explains why no difference was detected in the level of IL1β protein expressed in the wild type epidermis between basal

conditions and following exposure to TPA (Fig. 3B), despite our previous evidence that TPA increased the expression of the transcript (Fig. 3A).

The secreted form of IL1, mostly IL1β, contributes to the recruitment of leukocytes (mainly neutrophils and macrophages) but also, acts on stromal and infiltrating cells to induce the production of inflammatory cytokines, including IL1β itself, to sustain and propagate the inflammatory reaction (27). Accordingly, a transient increase in the number of IL1β-positive cells was detected in the dermis of the skin exposed to TPA (Fig. 3D). Chronic cutaneous inflammation caused by long-term DMBA/TPA treatment correlated with the presence of a population of IL1β-positive cells permanently residing in the dermis (Fig. 3D). In contrast, and consistent with impaired IL1β secretion, no infiltrating IL1β-positive cells were detected in the dermis of the mutant skin exposed to short-term TPA treatment or subjected to the two-stage chemical carcinogenesis protocol for 20 weeks (Fig 3D). Based on these results, we concluded that ERK5-dependent release of IL1β in the epidermis was required for promoting a secondary inflammatory reaction in the dermis.

To confirm that increased IL1β expression in the epidermis was a primary response to ERK5 activation in keratinocytes exposed to TPA, we undertook an analysis of ERK5 function in HaCat cells, a human immortalized keratinocyte cell line, to reproduce *in vitro* the immune response defect associated with the epidermal loss of ERK5 *in vivo*. We demonstrated that TPA stimulation induced phosphorylation of ERK5, as indicated by an electrophoretic mobility shift of the protein analyzed by immunoblot, and increased ERK5 activity (Fig. 4A). This was prevented by pre-incubating the cells with the pharmacological inhibitor of ERK5, XMD8-92 (Fig. 4A). Using this model system we confirmed the requirement of ERK5 in mediating TPA-induced up-regulation of *IL8* (the functional homolog of murine CXCL1/2), and *IL1*β, but not *TNF*α, mRNA (Fig. 4B). Next, HaCat cells were incubated with a caspase 1 inhibitor (YVAD-CHO) to prevent pro-IL1β from being cleaved and secreted (Fig. 4C). Under these conditions, we could detect TPA-mediated increased expression of pro-IL1β protein (Fig. 4C). This was prevented by pre-incubating the cells with XMD8-92 (Fig. 4C). Likewise, inhibition of ERK5 significantly reduced the amount of IL1β released in the media from cells treated with TPA (Fig 4D). Accordingly, ERK5 activation was required for both TPA-induced increased caspase 1 activity (Fig. 4E) and the proteolytic cleavage of caspase 1 to its active form (p20) (Fig. 4F). Together, these results firmly established that ERK5 was essential for IL1β production by keratinocytes and revealed a novel role for ERK5 in the regulation of IL1β signaling and IL8 expression in human cells.

ERK5 constitutes a novel therapeutic target to treat inflammation-driven cancer

To investigate whether our findings could be translated into a useful approach for cancer treatment, we examined the phenotypic consequence of the epidermal loss of ERK5 expression in skin tumors. We found that, under low tumor burden, the loss of ERK5 in neoplastic keratinocytes halted tumor growth induced by bi-weekly exposure to TPA (Fig. 5A). This was associated with a reduction in the number of proliferating cells labeled with BrdU, together with a collapse of tumor architecture (Fig. 5B). To determine whether an anti-ERK5 therapy could also block the growth of more advanced tumors, a similar

experiment was performed in cohorts of animals exhibiting a high tumor burden prior to disrupting ERK5 function by either *erk5* gene deletion or XMD8-92 treatment (Fig. 5C and D). We demonstrated that XMD8-92 effectively blocked TPA-induced ERK5 activation in the skin (Supplementary Fig. S2A). Moreover, like genetic deletion, pharmacological inhibition of ERK5 activity caused by exposing the skin to XMD8-92 prevented increased epidermal cell proliferation (Supplementary Fig. S2B), cells from infiltrating the dermis (Supplementary Fig. S2C), and increased caspase 1-mediated IL1β cleavage (Supplementary Fig. S2D and E) in response to TPA stimulation.

As expected, the number of papillomas larger than 3 mm in size increased over the time course of TPA treatment. Although this was not prevented by the genetic loss of *erk5*, representative pictures show that tumors were noticeably smaller in $erk5^{\Delta epidermis}$ than in $erk5^{wt}$ mice (Fig 5C). Likewise, exposure of the mouse skin to XMD8-92 affected tumor development with quantitative evidence of halted tumor growth (Fig. 5D). In contrast to the genetic strategy which permits the specific loss of ERK5 in keratinocytes, XMD8-92 will inhibit ERK5 activity in all cell types present in the epidermal and dermal compartments of the skin, including immune cells. This could explain the stronger effect of the inhibitor on tumor growth. However, we cannot exclude the possibility that the compound may exert some of its effect by partially inhibiting additional protein kinases involved in the inflammatory reaction.

Many effective anti-cancer regimens utilize more than one therapeutic agent. Therefore, we sought to explore the possibility that targeting ERK5 signaling could enhance the effectiveness of existing chemotherapeutic drugs. We employed a sub-therapeutic dosing regimen of chemotherapy (doxorubicin; 1.25 mg/kg weekly intravenous injection for 4 consecutive weeks) that exerted a limited effect on tumor growth, comparable to that caused by *erk5* gene deletion in mice harboring a high tumor burden (Fig. 5C). Importantly, mice subjected to this low-dose doxorubicin did not display gastro-intestinal side effects and weight loss exhibited by littermates receiving high-dose doxorubicin (2.5 mg/kg weekly intravenous injection for 4 consecutive weeks). We found that epidermal *erk5* gene deletion or XMD8-92 therapy combined with doxorubicin had an additive effect in preventing tumor growth, with evidence of tumor regression indicated by decreased number of large tumors (Fig. 6A and B). This is substantiated by the demonstration that the functional disruption of ERK5 signaling in mice concurrently treated with doxorubicin severely affected tumor architecture and markedly reduced the number of proliferating cells in the tumors (Fig. 6C).

Based on our previous results, we examined whether the effectiveness of anti-ERK5 therapy in regressing existing tumors was attributable to the requirement of ERK5 for sustained inflammation in the skin. This hypothesis was confirmed by evidence that the loss of ERK5 expression (Fig. 7A) or activity (Fig. 7B) was associated with a significant reduction in the number of neutrophils (MPO-positive cells) infiltrating the neoplastic epidermis (E) and the tumor stroma (S), independently of doxorubicin treatment. This correlated with a decreased number of mast cells (toluidine blue-stained cells) present in the tumor stroma (Fig. 7A and B). These results are consistent with evidence that persistent neutrophil and mast cells recruitment is required for tumor maintenance (16). Furthermore, tumors displayed strong and diffuse IL1β staining in the papilloma epithelium (E), indicative of IL1β secretion in the

tumor microenvironment (Fig. 7A and B). This was accompanied by an influx of IL1β-positive cells in the tumor stroma (S) (Fig. 7A and B). A reduction in both, IL1β secretion and the number of IL1β-positive cells was observed following the functional disruption of ERK5 signaling, thereby demonstrating the requirement of ERK5 for continued IL1β production in established tumors (Fig. 7A and B). Importantly, none of these inflammatory markers were affected by doxorubicin treatment alone.

Together, these results indicate that neutralizing inflammation by blocking ERK5 in existing tumors represents a novel strategy by which to treat CRI. Additionally, we demonstrate that combining anti-ERK5 therapy with chemotherapeutic agents augments the anti-tumorigenic effect of anti-ERK5 treatment whilst concurrently lowering the therapeutic threshold of these agents, consequently reducing associated side effects.

DISCUSSION

We have discovered that epidermal expression of ERK5 is required for mediating inflammation in the skin. Furthermore, we have demonstrated that inactivation of ERK5 in epidermal keratinocytes prevented inflammation-driven tumorigenesis, with evidence that ERK5 is critical for the development of skin squamous cell carcinomas (SCC). SCC is one of the most common types of human non-melanoma skin cancer (28). The lesions arise from keratinocytes in sun-exposed areas of the epidermis and are characterized by an increased risk of metastasis compared to basal cell carcinomas. Therefore, these findings are highly relevant because elevated MEK5/ERK5 expression in human epithelial tumors correlates with unfavorable prognosis (9). Additionally, inflammation is a hallmark of most, if not all, cancer (4). In particular, besides ultraviolet light, inflammatory skin diseases also predispose patients to developing cutaneous SCC (28). Accordingly, targeting CRI has become one of the best options by which to advance cancer treatment. This therapeutic strategy is already supported by evidence that tumor burden can be reduced in mice in which key mediators of the immune response are blocked by genetic or pharmacological means (2). Importantly, several cytokine antagonists are being tested in phase II clinical trials with some encouraging results (2).

The idea that ERK5 provides a mechanistic link between inflammation and cancer originated from our observation that the migration of neutrophils and mast cells to the skin, after short and long term exposure to TPA, was impaired in the absence of epidermal ERK5. Likewise, the functional inhibition of ERK5 in the neoplastic epidermis correlated with a significant reduction in the number of infiltrating neutrophils and mast cells in all tumor compartments. The recruitment of neutrophils in inflamed skin is regulated by chemokines, notably CXCL1 and CXCL2, which signal through the same receptor, CXCR2. Like *erk5* gene deletion, CXCR2 deficiency was shown to suppress inflammation-driven tumorigenesis (18, 19) and it was postulated that CXCR2-driven neutrophil recruitment stimulates epithelial cell proliferation in the skin (19). Furthermore, depletion of $Ly6G^{+}$ cells, which include neutrophils, was associated with increased tumor cell death (19). Therefore, it is reasonable to propose that the up-regulation of CXCL1 and CXCL2 constitutes an important mechanism by which ERK5 triggers the neutrophilic inflammation required for tumor cell proliferation and viability.

The causal relationship between ERK5 and inflammation is further supported by the demonstration that epidermal ERK5 controls the expression of a specific subset of pro-inflammatory mediators currently under pre-clinical therapeutic investigation for the treatment of human cancer (2). In particular, the functional loss of ERK5 in keratinocytes prevented TPA-induced up-regulation of *IL1*α, *IL1*β and *COX-2* transcripts. However, in contrast to malignant mesothelioma cell lines (29), we found no evidence that epidermal ERK5 was required for *IL6* gene expression. This may reflect a cell specific function of ERK5 at various stages of malignant transformation. Likewise, no difference was observed in the level of *TNF*α mRNA between wild type and ERK5-deficient epidermis under basal or stimulated conditions. Mice lacking TNFα have been reported to be resistant to the development of skin tumor induced by DMBA/TPA (30, 31). However, TNF receptor deficiency does not prevent neutrophil infiltration in the epidermis exhibiting increased PKCα activity (32). Therefore, our findings are consistent with the idea that TNFα does not contribute to ERK5-mediated recruitment of neutrophils in the skin exposed to inflammatory stimuli.

Recently, autocrine activation of NFκB through an IL1 receptor-MyD88 axis has emerged as an essential positive feedback loop that reinforces the expression of pro-tumorigenic factors in Ras-transformed keratinocytes (6). Importantly, targeted deletion of the *MyD88* gene in keratinocytes conferred a significant resistance of the skin to DMBA/TPA-induced tumorigenesis, thereby confirming the important contribution of epidermal IL1 signaling in cancer (6). However, while transformation by oncogenic Ras induced both *IL1*α and *IL1β* mRNA, IL1β was undetectable in the culture supernatants (6). Therefore, we can speculate that increased caspase 1 activity, caused by elevated ERK5 signaling in keratinocytes, independently of oncogenic mutation, may be sufficient to trigger a non-resolving inflammatory condition that increases cancer risk. This raises the interesting possibility of potential prophylactic applications for anti-ERK5 therapy in cancer development. Furthermore, consistent with the requirement of ERK5 for caspase 1-mediated cleavage of pro-IL1β, tumor regression associated with the epidermal loss of ERK5 was accompanied with the depletion of secreted IL1β in the papilloma epithelium. It is well established that IL1β can act on stromal cells (fibroblasts and inflammatory cells) to induce the production of a cascade of inflammatory cytokines but also, adhesion molecules and angiogenic factors to increase tumor invasiveness and metastasis (27, 33). Therefore, impairing tumoral IL1β signaling via anti-ERK5 therapy may also yield therapeutic results in the prevention of metastatic progression.

Collectively, genetic evidence that the functional loss of ERK5 in keratinocytes causes, simultaneously, the down-regulation of several inflammatory mediators over-expressed in various human cancers, suggest that an anti-ERK5 therapy may have the potential to be clinically more efficacious than therapies directed against individual inflammatory mediators. Furthermore, the pathway organized in a typical three-tiered kinase (MAPKKK, MAPKK, MAPK) cascade offers multiple potential targets, highly suitable for drug design. In particular, an alternative therapeutic strategy targeting MEK5, instead of ERK5, may allow the specific inhibition of pathological ERK5 activation with reduced undesirable side effects. Indeed, whilst the systemic administration of XMD8-92, a selective and potent ATP-

competitive inhibitor of ERK5 had no apparent adverse effects in mice, the specific loss of ERK5 signaling in endothelial cells during embryogenesis or in adult mice resulted in lethality as a consequence of vascular instability (8, 34). A similar approach has been employed for the ERK1/2 MAPK signaling pathway, where most current efforts target their upstream activators, namely MEK1/2, rather than inhibiting ERK1/2 directly. A clinical study involving cancer patients has confirmed decreased ERK1/2 phosphorylation in tumors and several partial remissions when MEK1/2 were inhibited (35). Hence, the rationale for MAPK kinase blockade in humans is quite clear.

To conclude, we propose that ERK5 is part of a core signal transduction pathway that drives the expression of a specific subset of inflammatory mediators in epithelial cells that can act in an autocrine and paracrine manner to initiate an immune response. As such, anti-ERK5 therapy provides a new opportunity to neutralize inflammation associated with cancer.

Supplementary Material

Refer to Web version on PubMed Central for supplementary material.

ACKNOWLEDGEMENTS

We thank Peter March (Bioimaging Facility, University of Manchester) for very helpful advice with the microscopy and the staff at the University of Manchester Biological Services Facility for looking after the mice. The authors declare no conflict of interest.

Financial support: This work was supported by grants mainly from Worldwide Cancer Research (10-0134) and partly from Cancer Research UK (C18267/A11727) and the Wellcome Trust (097820/Z/11/B).

REFERENCES

1. Mantovani A, Allavena P, Sica A, Balkwill F. Cancer-related inflammation. Nature. 2008; 454:436–44. [PubMed: 18650914]
2. Balkwill FR, Mantovani A. Cancer-related inflammation: common themes and therapeutic opportunities. Semin Cancer Biol. 2012; 22:33–40. [PubMed: 22210179]
3. DeNardo DG, Brennan DJ, Rexhepaj E, Ruffell B, Shiao SL, Madden SF, et al. Leukocyte complexity predicts breast cancer survival and functionally regulates response to chemotherapy. Cancer Discov. 2011; 1:54–67. [PubMed: 22039576]
4. Mantovani A. Cancer: Inflaming metastasis. Nature. 2009; 457:36–7. [PubMed: 19122629]
5. Grivennikov SI, Greten FR, Karin M. Immunity, inflammation, and cancer. Cell. 2010; 140:883–99. [PubMed: 20303878]
6. Cataisson C, Salcedo R, Hakim S, Moffitt BA, Wright L, Yi M, et al. IL-1R-MyD88 signaling in keratinocyte transformation and carcinogenesis. J Exp Med. 2012; 209:1689–702. [PubMed: 22908325]
7. Hayashi M, Fearns C, Eliceiri B, Yang Y, Lee JD. Big mitogen-activated protein kinase 1/extracellular signal-regulated kinase 5 signaling pathway is essential for tumor-associated angiogenesis. Cancer Res. 2005; 65:7699–706. [PubMed: 16140937]
8. Yang Q, Deng X, Lu B, Cameron M, Fearns C, Patricelli MP, et al. Pharmacological inhibition of BMK1 suppresses tumor growth through promyelocytic leukemia protein. Cancer Cell. 2010; 18:258–67. [PubMed: 20832753]
9. Lochhead PA, Gilley R, Cook SJ. ERK5 and its role in tumour development. Biochem Soc Trans. 2012; 40:251–6. [PubMed: 22260700]

10. Finegan KG, Wang X, Lee EJ, Robinson AC, Tournier C. Regulation of neuronal survival by the extracellular signal-regulated protein kinase 5. Cell Death Differ. 2009; 16:674–83. [PubMed: 19148185]
11. Finegan KG, Tournier C. The mitogen-activated protein kinase kinase 4 has a pro-oncogenic role in skin cancer. Cancer Res. 2010; 70:5797–806. [PubMed: 20610622]
12. Kayahara M, Wang X, Tournier C. Selective regulation of c-jun gene expression by mitogen-activated protein kinases via the 12-o-tetradecanoylphorbol-13-acetate-responsive element and myocyte enhancer factor 2 binding sites. Mol Cell Biol. 2005; 25:3784–92. [PubMed: 15831482]
13. Hayashi M, Lee JD. Role of the BMK1/ERK5 signaling pathway: lessons from knockout mice. J Mol Med (Berl). 2004; 82:800–8. [PubMed: 15517128]
14. Indra AK, Li M, Brocard J, Warot X, Bornert JM, Gerard C, et al. Targeted somatic mutagenesis in mouse epidermis. Horm Res. 2000; 54:296–300. [PubMed: 11595821]
15. Abel EL, Angel JM, Kiguchi K, DiGiovanni J. Multi-stage chemical carcinogenesis in mouse skin: fundamentals and applications. Nat Protoc. 2009; 4:1350–62. [PubMed: 19713956]
16. Mueller MM. Inflammation in epithelial skin tumours: old stories and new ideas. Eur J Cancer. 2006; 42:735–44. [PubMed: 16527478]
17. Hennings H, Shores R, Wenk ML, Spangler EF, Tarone R, Yuspa SH. Malignant conversion of mouse skin tumours is increased by tumour initiators and unaffected by tumour promoters. Nature. 1983; 304:67–9. [PubMed: 6866091]
18. Cataisson C, Ohman R, Patel G, Pearson A, Tsien M, Jay S, et al. Inducible cutaneous inflammation reveals a protumorigenic role for keratinocyte CXCR2 in skin carcinogenesis. Cancer Res. 2009; 69:319–28. [PubMed: 19118017]
19. Jamieson T, Clarke M, Steele CW, Samuel MS, Neumann J, Jung A, et al. Inhibition of CXCR2 profoundly suppresses inflammation-driven and spontaneous tumorigenesis. J Clin Invest. 2012; 122:3127–44. [PubMed: 22922255]
20. Cataisson C, Pearson AJ, Tsien MZ, Mascia F, Gao JL, Pastore S, et al. CXCR2 ligands and G-CSF mediate PKCalpha-induced intraepidermal inflammation. J Clin Invest. 2006; 116:2757–66. [PubMed: 16964312]
21. Coussens LM, Raymond WW, Bergers G, Laig-Webster M, Behrendtsen O, Werb Z, et al. Inflammatory mast cells up-regulate angiogenesis during squamous epithelial carcinogenesis. Genes Dev. 1999; 13:1382–97. [PubMed: 10364156]
22. Gabay C, Lamacchia C, Palmer G. IL-1 pathways in inflammation and human diseases. Nat Rev Rheumatol. 2010; 6:232–41. [PubMed: 20177398]
23. Rundhaug JE, Simper MS, Surh I, Fischer SM. The role of the EP receptors for prostaglandin E2 in skin and skin cancer. Cancer Metastasis Rev. 2011; 30:465–80. [PubMed: 22012553]
24. Lee JL, Kim A, Kopelovich L, Bickers DR, Athar M. Differential expression of E prostanoid receptors in murine and human non-melanoma skin cancer. J Invest Dermatol. 2005; 125:818–825. [PubMed: 16185283]
25. Dinarello CA. IL-1: discoveries, controversies and future directions. Eur J Immunol. 2010; 40:599–606. [PubMed: 20201008]
26. Eder C. Mechanisms of interleukin-1beta release. Immunobiology. 2009; 214:543–53. [PubMed: 19250700]
27. Apte RN, Dotan S, Elkabets M, White MR, Reich E, Carmi Y, et al. The involvement of IL-1 in tumorigenesis, tumor invasiveness, metastasis and tumor-host interactions. Cancer Metastasis Rev. 2006; 25:387–408. [PubMed: 17043764]
28. Ratushny V, Gober MD, Hick R, Ridky TW, Seykora JT. From keratinocyte to cancer: the pathogenesis and modeling of cutaneous squamous cell carcinoma. J Clin Invest. 2012; 122:464–72. [PubMed: 22293185]
29. Shukla A, Miller JM, Cason C, Sayan M, Macpherson MB, Beuschel SL, et al. Extracellular signal-regulated kinase 5: a potential therapeutic target for malignant mesotheliomas. Clin Cancer Res. 2013; 19:2071–83. [PubMed: 23446998]
30. Moore RJ, Owens DM, Stamp G, Arnott C, Burke F, East N, et al. Mice deficient in tumor necrosis factor-alpha are resistant to skin carcinogenesis. Nat Med. 1999; 5:828–31. [PubMed: 10395330]

31. Suganuma M, Okabe S, Marino MW, Sakai A, Sueoka E, Fujiki H. Essential role of tumor necrosis factor alpha (TNF-alpha) in tumor promotion as revealed by TNF-alpha-deficient mice. Cancer Res. 1999; 59:4516–8. [PubMed: 10493498]

32. Cataisson C, Pearson AJ, Torgerson S, Nedospasov SA, Yuspa SH. Protein kinase C alpha-mediated chemotaxis of neutrophils requires NF-kappa B activity but is independent of TNF alpha signaling in mouse skin in vivo. J Immunol. 2005; 174:1686–92. [PubMed: 15661932]

33. Voronov E, Shouval DS, Krelin Y, Cagnano E, Benharroch D, Iwakura Y, et al. IL-1 is required for tumor invasiveness and angiogenesis. Proc Natl Acad Sci U S A. 2003; 100:2645–50. [PubMed: 12598651]

34. Hayashi M, Kim SW, Imanaka-Yoshida K, Yoshida T, Abel ED, Eliceiri B, et al. Targeted deletion of BMK1/ERK5 in adult mice perturbs vascular integrity and leads to endothelial failure. J Clin Invest. 2004; 113:1138–48. [PubMed: 15085193]

35. Kohno M, Tanimura S, Ozaki K. Targeting the extracellular signal-regulated kinase pathway in cancer therapy. Biol Pharm Bull. 2011; 34:1781–4. [PubMed: 22130230]

Europe PMC Funders Author Manuscripts

Europe PMC Funders Author Manuscripts

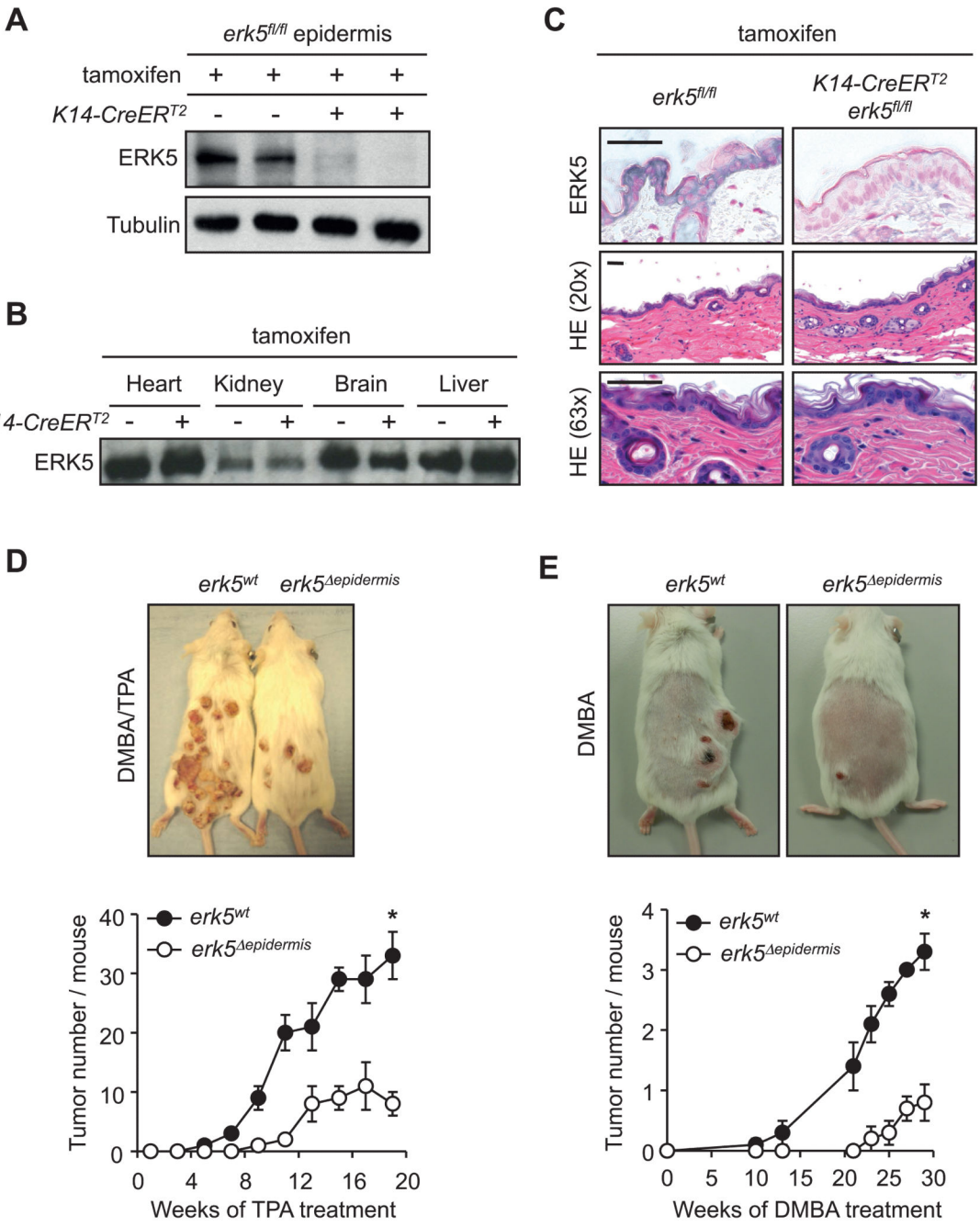

Figure 1.

ERK5 is required for skin tumor formation. Adult *erk5*$^{fl/fl}$ mice carrying (+) or not (−) the *K14-CreER*^{T2} transgene were subjected to intra-peritoneal tamoxifen injections. **A** and **B**, The specific inactivation of the *erk5* gene in the epidermis of mice expressing CreER^{T2} was confirmed by immunoblot analyses and **C**, by immunostaining of skin biopsies with a specific antibody to ERK5 (gray). Slides were counterstained with nuclear red. HE staining indicates that the absence of ERK5 does not disrupt the architecture of the skin. **D** and **E**, Representative pictures of mice bearing papillomas 20 weeks after DMBA/TPA treatment

(D) and of mice bearing SCC 29 weeks after repeated exposure to DMBA (E). Papillomas or SCC growing on the back skin of mice exposed to DMBA/TPA or DMBA alone were counted. The data are represented as average number of tumors per mice ± SE. Total number of animals used was 60 in panel D and 16 in panel E.

Europe PMC Funders Author Manuscripts

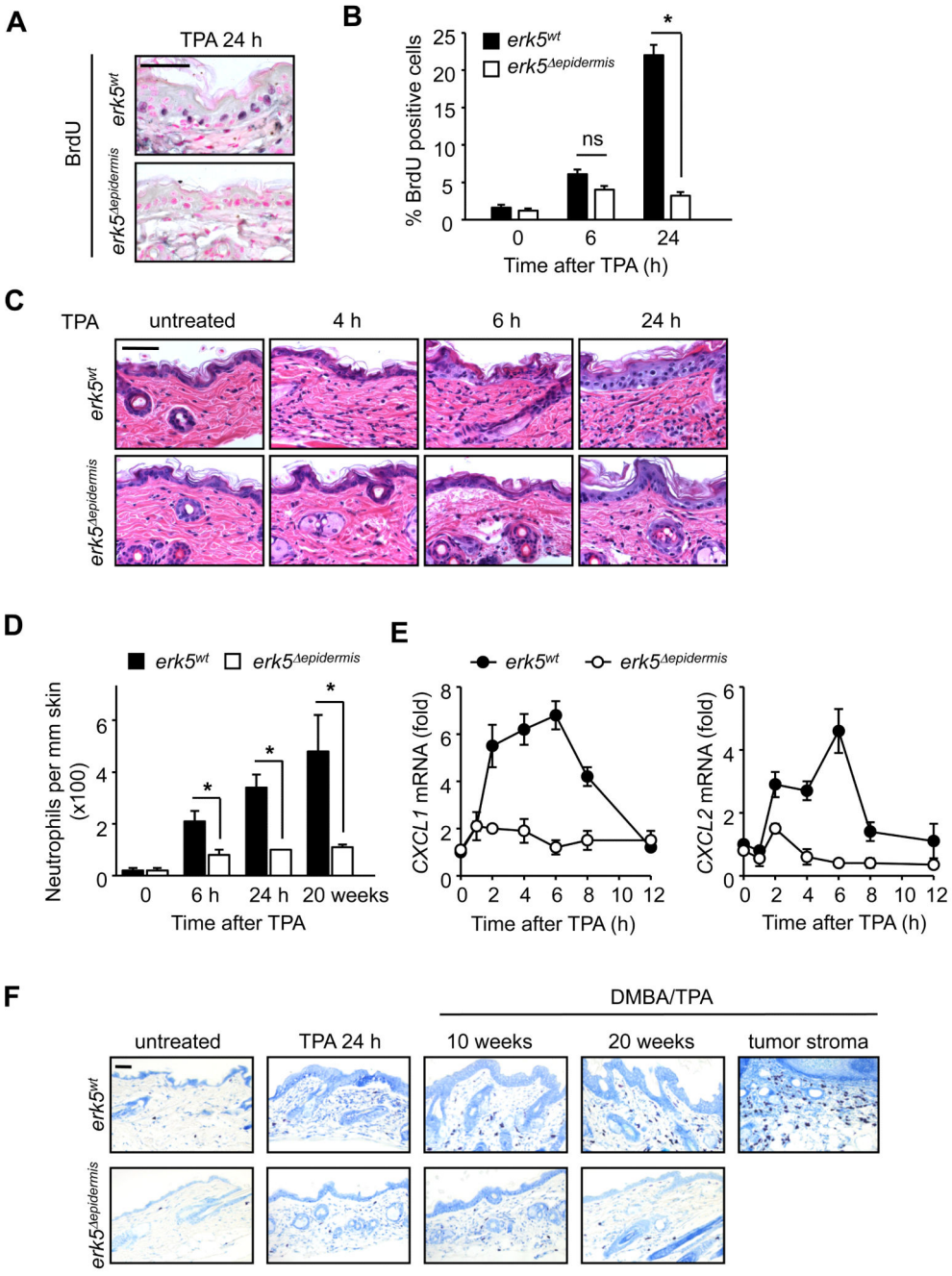

Figure 2.

erk5 gene deletion reduces TPA-induced inflammation. Dorsal skins of *erk5*^{wt} and *erk5*$^{\Delta epidermis}$ mice were exposed to TPA or DMBA/TPA for the indicated times. **A** and **B**, Mice exposed to a single dose of TPA were injected intraperitoneally with BrdU 1 h prior to the end of treatment. Skin biopsies were processed for BrdU immunoreactivity. Positive cells are stained in grey (A). Slides were counterstained with nuclear red. The number of BrdU-positive cells per 100 cells in 10 fields per section was blind counted by 2 users and the average number recorded (B). The experimental mean ± SE was generated from 16

slides (4 sections from 4 mice). **C**, HE staining of skin biopsies shows that the dermis of the mutant skin displays a marked defect in inflammatory cell infiltration following TPA treatment. **D**, The number of neutrophils in the skin after TPA treatment was estimated by quantitative analysis of MPO-positive cells. The experimental mean ± SE was generated from 8 slides (2 sections from 4 mice). **E**, Total RNA was extracted from epidermises and the amount of *CXCL1* and *CXCL2* transcripts was measured by quantitative real-time PCR. The data correspond to the mean ± SE of 3 independent experiments in which 1 mouse was used per experimental condition. Total number of animals used in this panel was 42. **F**, Chronic inflammation was assessed in skin biopsies by toluidine blue staining of mast cells. Scale bars, 50 μm.

Europe PMC Funders Author Manuscripts

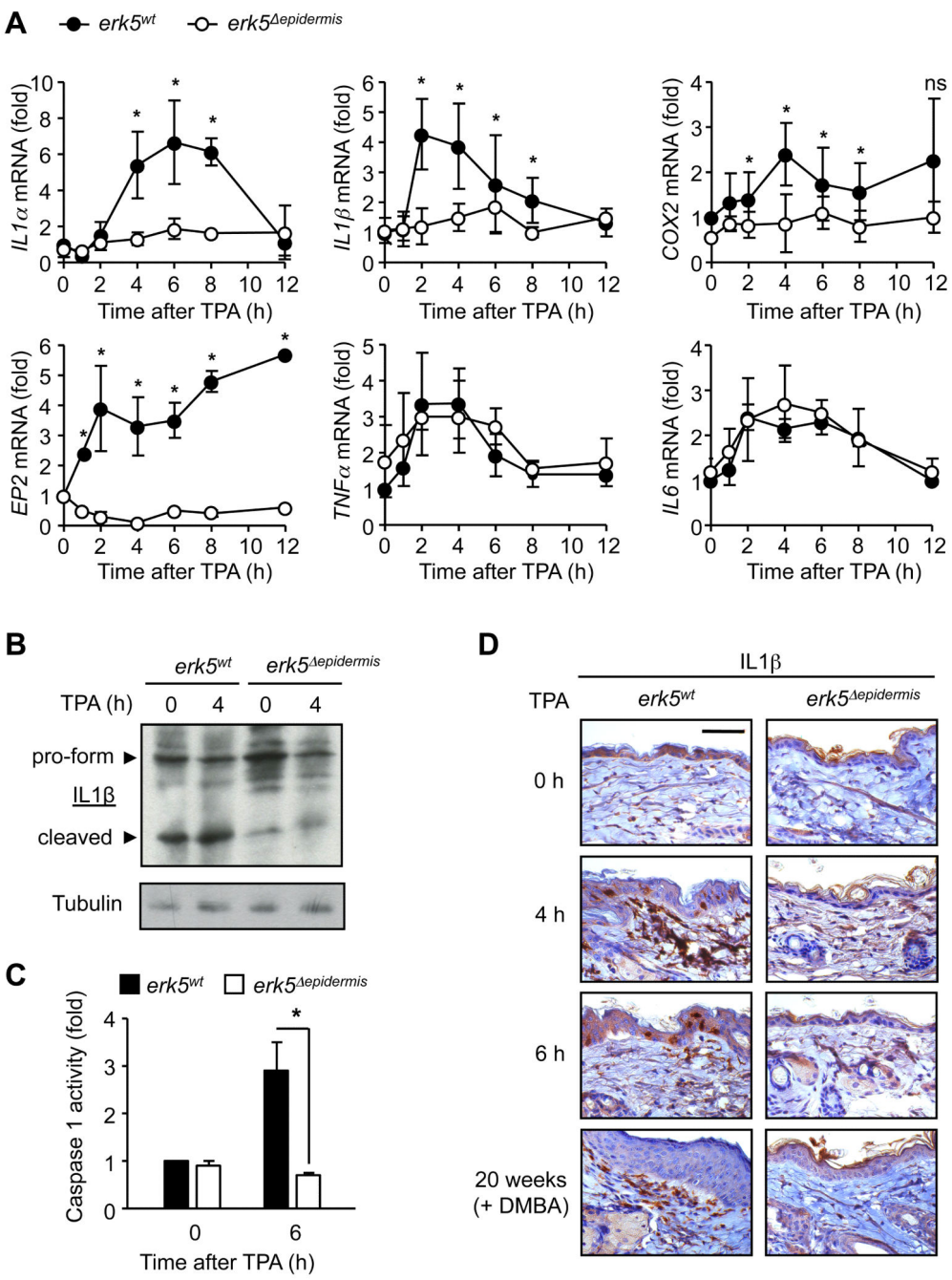

Figure 3.

In vivo regulation of pro-inflammatory cytokines by ERK5. Dorsal skins of *erk5*^{wt} and *erk5*$^{\Delta epidermis}$ mice were exposed to TPA or DMBA/TPA for the indicated times. **A**, Total RNA was extracted from epidermises and the amount of transcripts was measured by quantitative real-time PCR. The data correspond to the mean ± SE of 3 independent experiments in which 1 mouse was used per experimental condition. Total number of animals used in this panel was 42. **B** and **D**, IL1β expression in skin biopsies was determined by immunoblot analysis (B) and by immunohistochemistry (D) with a specific antibody

against IL1β. Scale bar, 50 μm. **C**, Caspase 1 activity in epidermal extracts was measured by caspase assay. The data correspond to the mean ± SE of 3 independent experiments in which 1 mouse was used per experimental condition. Total number of animals used in this panel was 12.

Europe PMC Funders Author Manuscripts

Europe PMC Funders Author Manuscripts

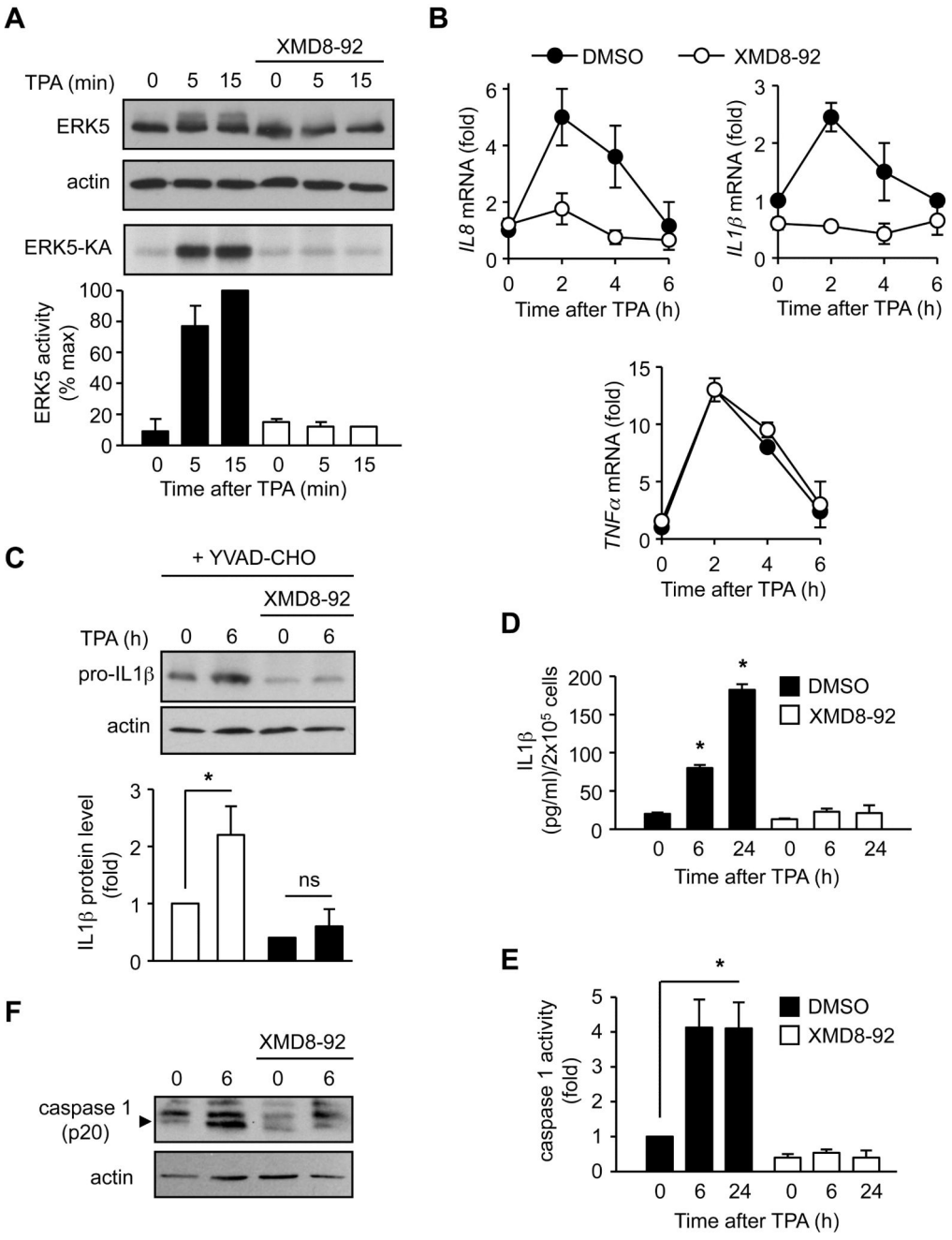

Figure 4.

Pharmacological inhibition of ERK5 in HaCat cells blocks IL1β secretion following TPA stimulation. HaCat cells were mock treated (DMSO) or treated with XMD8-92 prior to being incubated with TPA for the indicated times. **A**, The effect of TPA treatment on ERK5 expression and post-translational modification was examined by immunoblot analysis. Similar results were obtained in two independent experiments. Endogenous ERK5 activity was measured by protein kinase assay (KA). The radioactivity incorporated in the GST-MEF2 substrate was quantified by phosphoImager. The data correspond to the mean ± SE of

three independent experiments. **B**, Total RNA was extracted and the level of *IL8*, *IL1β* and *TNF*α transcripts was quantitated by real-time PCR. The data correspond to the mean ± SE of three independent experiments performed in triplicate. **C**, Caspase 1 activity was inhibited by incubating the cells with YVAD-CHO. Protein lysates were analyzed by immunoblot with an antibody against IL1β. Signals corresponding to the pro-IL1β protein were quantified with the ImageQuantifier software (BioImage, Jackson MI). The data correspond to the mean ± SE of three independent experiments. **D**, The amount of IL1β released in culture supernatants was measured by ELISA. The data correspond to the mean ± SE generated from three independent experiments performed in triplicate. **E**, Caspase 1 activity was measured by caspase assay. The data correspond to the mean ± SE generated from three independent experiments performed in triplicate. **F**, Protein lysates were analyzed by immunoblot with an antibody against caspase 1. Similar results were obtained in two independent experiments.

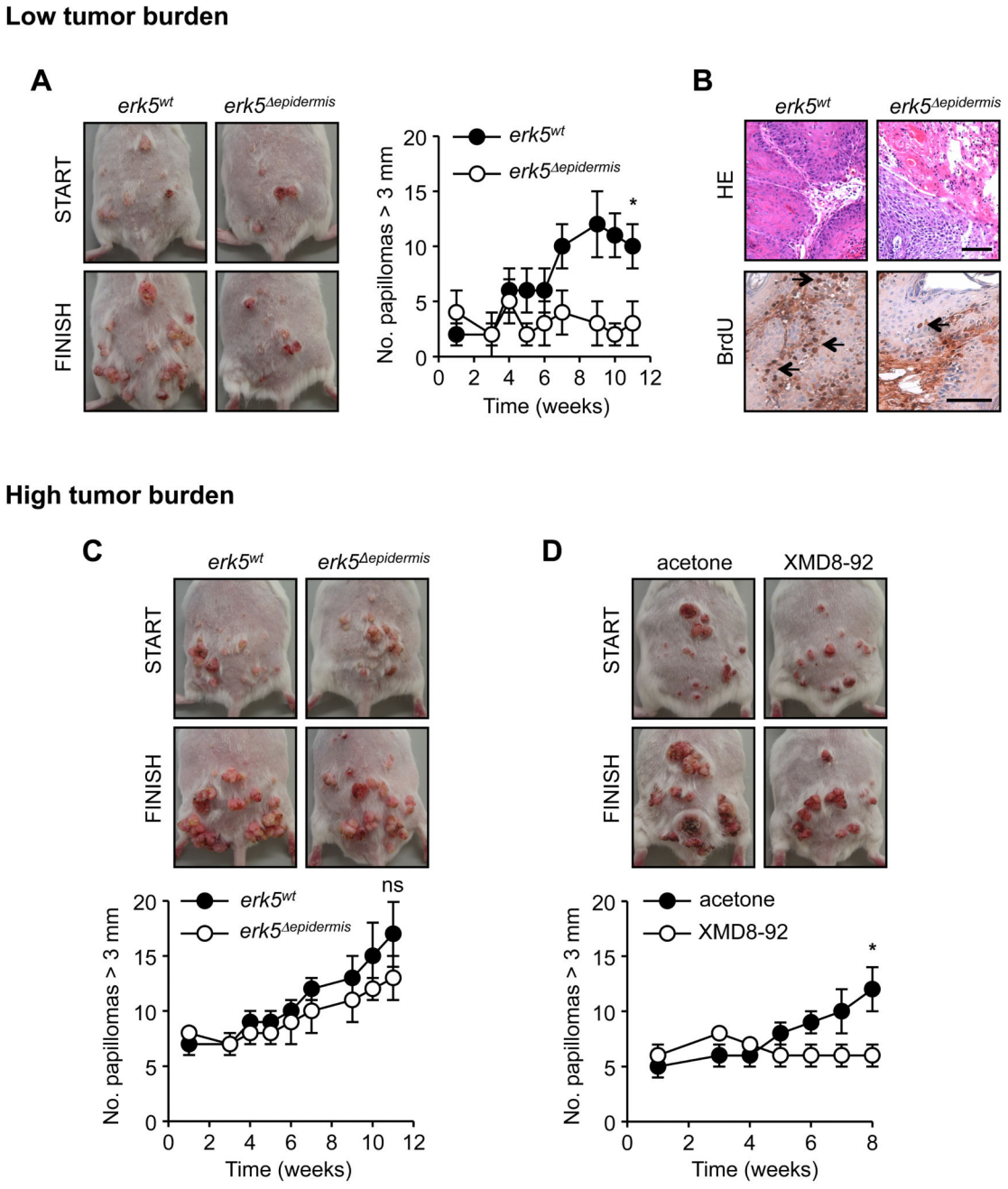

Figure 5.

The functional disruption of ERK5 blocks the growth of papillomas. *erk5*$^{fl/fl}$ and *K14-CreER*^{T2};*erk5*$^{fl/fl}$ littermates were subjected to the DMBA/TPA protocol until the appearance of papillomas (START). This took 10 weeks or 14-16 weeks for reaching low (A and B) or high (C and D) tumor burden, respectively. Mice were subsequently subjected to tamoxifen (A, B and C) to induce *erk5* gene deletion in neoplastic keratinocytes expressing Cre or treated with XMD8-92 **(D)** to inhibit ERK5 activity in the skin. Bi-weekly TPA administration was continued for a further 11 (tamoxifen) or 8 (XMD8-92) weeks (FINISH).

A, **C** and **D**, Representative images of the tumor burden exhibited by animals at the start and finish of the experiment. The number of tumors ≥ 3 mm in size was blind-recorded during the experiment. The data correspond to the mean ± SE of 3 independent experiments in which at least 6 wild type and 6 mutant animals were analyzed. Total number of animals used per panel was 36. **B**, Mice were injected intraperitoneally with BrdU 2 h prior to being sacrificed at the end of the experiment (FINISH). Representative sections of tumors stained with eosin or processed for BrdU immunoreactivity are shown. The slides were counterstained with hemotoxylin (blue). BrdU-positive cells (brown) are indicated with an arrow. Scale bars, 50 μm

Europe PMC Funders Author Manuscripts

Europe PMC Funders Author Manuscripts

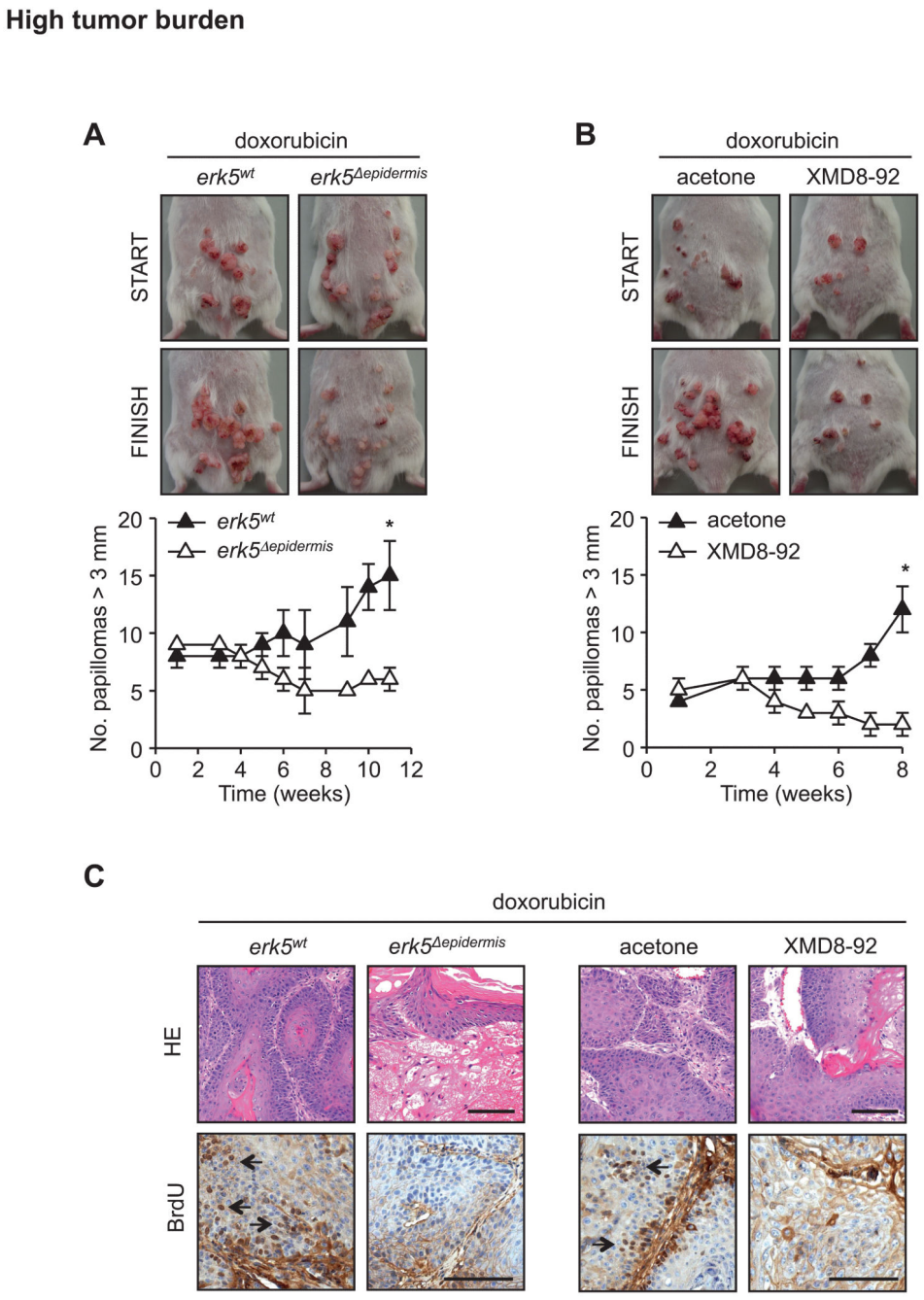

Figure 6.

The functional disruption of ERK5 signaling synergizes with sub-therapeutic doxorubicin treatment to decrease tumor burden. *erk5*$^{fl/fl}$ and *K14-CreER*^{T2};*erk5*$^{fl/fl}$ littermates were subjected to the DMBA/TPA protocol until the appearance of papillomas (14-16 weeks, START). Mice were subsequently subjected to tamoxifen (A and C) or XMD8-92 (B and C), together with doxorubicin. Bi-weekly TPA administration was continued for a further 11 (tamoxifen) or 8 (XMD8-92) weeks (FINISH). **A** and **B**, Representative images of the tumor burden exhibited by animals at the start and finish of the experiment. The number of tumors

≥ 3 mm in size was blind-recorded during the experiment. The data correspond to the mean ± SE of 3 independent experiments in which at least 6 wild type and 6 mutant animals were analyzed. Total number of animals used per panel was 36. **C,** Mice were injected intraperitoneally with BrdU 2 h prior to being sacrificed at the end of the experiment (FINISH). Representative sections of tumors stained with eosin or processed for BrdU immunoreactivity are shown. The slides were counterstained with hemotoxylin (blue). BrdU-positive cells (brown) are indicated with an arrow. Scale bars, 50 μm.

Europe PMC Funders Author Manuscripts

Europe PMC Funders Author Manuscripts

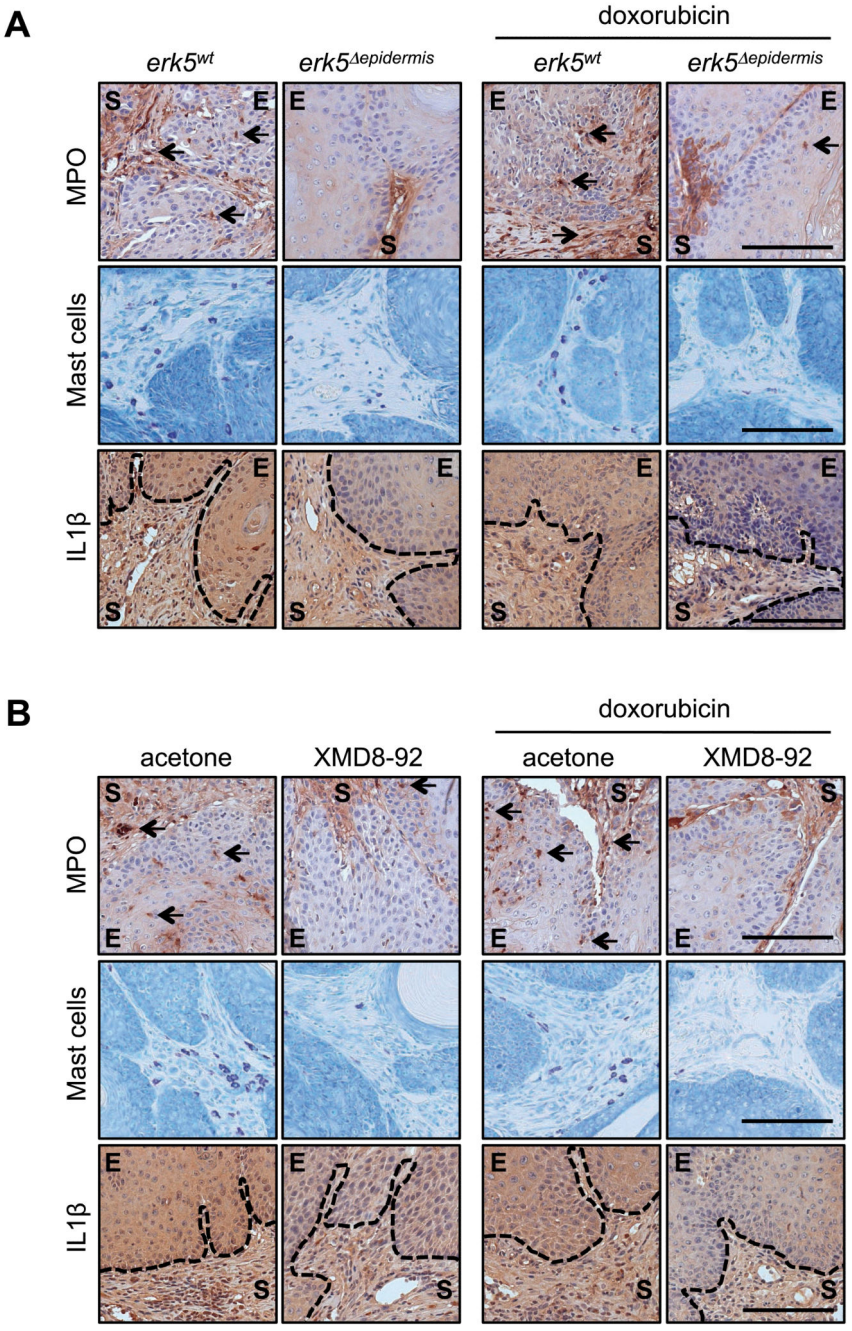

Figure 7.

Anti-ERK5 therapy neutralizes tumor-associated inflammation. *erk5*$^{fl/fl}$ and *K14-CreER*^{T2};*erk5*$^{fl/fl}$ littermates were subjected to the DMBA/TPA protocol until the appearance of papillomas (14-16 weeks). Mice were subsequently subjected to tamoxifen (A) or XMD8-92 (B), together without or with doxorubicin. Bi-weekly TPA administration was continued for a further 10 weeks. **A** and **B**, Immunohistochemical analysis of sections of tumors collected at the end of the experiment was performed with antibodies to MPO and IL1β. Arrows indicate positively stained neutrophils. Mast cells were detected by toluidine

blue staining. E, neoplastic epidermis; S, tumor stroma. The demarcation between these two compartments is indicated by a dashed line on IL1β-immunostained tumor sections. Scale bars, 50 μm.

Europe PMC Funders Author Manuscripts